Research Square

Preprints are preliminary reports that have not undergone peer review.
They should not be considered conclusive, used to inform clinical practice,
or referenced by the media as validated information.

Ligand exchange and stability of CdTe nanoplatelets under mild conditions

Dulat Daurenbekov
L. N. Gumilyov Eurasian National University
Aigerim Ospanova
aygerim-ospanova-00@mail.ru

L. N. Gumilyov Eurasian National University
Asset Kainarbay
L. N. Gumilyov Eurasian National University
Yerkebulan Koshkinbayev
L. N. Gumilyov Eurasian National University
Mekhrdod S. Kurboniyon
Chongqing University of Posts and Telecommunications
Rakhima Daurenbekova
L. N. Gumilyov Eurasian National University
Aizhan Akhmetova
L. N. Gumilyov Eurasian National University
Alexander Vinokurov
Lomonosov Moscow State University
Sergey Dorofeev
Lomonosov Moscow State University
Sergei Bubenov
Lomonosov Moscow State University

Article

Keywords: nanoplatelets, CdTe, ligand exchange, photoluminescence, hexadecanthiol, stoichiometry

Posted Date: June 26th, 2026

DOI: https://doi.org/10.21203/rs.3.rs-10020395/v1

License: This work is licensed under a Creative Commons Attribution 4.0 International License.
Read Full License

Additional Declarations: No competing interests reported.

Abstract

CdTe colloidal nanoplatelets (NPLs) are promising two-dimensional quantum emitters, but their optical response remains highly sensitive to surface chemistry and post-synthetic processing. In this work, we examine how precursor stoichiometry and mild ligand-exchange conditions affect the optical stability of CdTe NPLs synthesized at 170°C. By varying the Cd and Te precursor concentrations by ± 50% relative to the standard protocol, we identified a precursor-composition window in which the characteristic excitonic absorption features of ~ 3 ML CdTe NPLs appear rapidly during the early stages of growth. TXRF analysis of purified NPL fractions showed slightly Cd-rich compositions, with Cd/Te ratios ranging from 1.03 to 1.19, consistent with Cd-terminated surfaces stabilized by carboxylate ligands. The optical properties were evaluated by absorption, photoluminescence, and photoluminescence quantum yield measurements, while repeated measurements after storage were used to assess the reliability of the spectral features and the long-term evolution of emission. The main excitonic emission was retained after storage, although an increased long-wavelength contribution indicated partial optical aging of selected samples. We further tested three ligand-exchange strategies commonly used for CdSe-based nanocrystals: carboxylate-to-$CdCl_2$, carboxylate-to-$Zn(DDTC)_2$, and carboxylate-to-hexadecanethiol exchange. $CdCl_2$ and $Zn(DDTC)_2$ treatments did not produce measurable shifts of the excitonic transitions and led to colloidal destabilization under the applied conditions, whereas hexadecanethiol treatment produced clear surface-related optical changes. These results show that CdTe NPLs can preserve their excitonic optical signature under selected mild post-synthetic conditions, but their surface chemistry is less tolerant to CdSe-derived ligand-exchange protocols than expected.

1. Introduction

Over the past decade, colloidal nanoplatelets made of II–VI semiconductors (e.g., CdSe and CdTe) have become a recognized type of two-dimensional quantum nanocrystals. Their unique properties—precisely controllable thickness at the atomic level, narrow exciton transitions, and high oscillatory strength—make them promising for use in various optoelectronic devices, such as LEDs, lasers, photodetectors, and scintillators [1–6]. Among these, CdTe nanoplatelets are particularly interesting due to their narrow band gap, strong absorption, and existing technologies for their application in thin-film solar cells [2,7–10]. Recent studies have shown that varying the synthesis temperature allows for precise tuning of their thickness, and composition, which directly affects their optical properties [11,12].

The influence of surface ligands on the optical and structural properties of CdTe nanoplatelets (NPLs) and their films has not been sufficiently studied, especially compared to similar studies for CdSe [13–15]. Notably, ligand exchange, for example with alkyl thiols, can induce spontaneous folding of CdTe nanosheets into tubular and helical structures, leading to significant changes in their morphology and packing [16]. In the principal confinement direction the NPLs are thinner than quantum dots, so a larger portion of the inorganic core constituent atoms is surface-adjacent Consequently, the structural and optical properties of NPLs are primarily determined by surface ligands [17].

The colloidal stability and controlled particle growth of widely used Cd-containing NPLs are ensured by their typical initial shell, consisting of carboxylate ligands such as oleate or propionate [1,11]. However, as many studies demonstrate, even minor modifications in the chemical environment of the ligand can significantly affect the spectral characteristics of the emission (making the lines broader or narrower), change the lifetime of excited states (excitons), and promote the formation of defects on the surface [17]. Fine-tuning of the properties of colloidal nanocrystals depends on postsynthetic ligand exchange [18,19]. The transition from carboxylate to thiol ligands is of considerable research interest. This is due to the fact that the relatively soft acidity of cadmium cations promotes the thermodynamic stability of the Cd–S bond. Furthermore, thiolate ligands have the unique ability to form a variety of surface structures: from ordered monomolecular layers to multilayered, more complex sulfur-containing shells [19].

While the mechanism of CdTe NPL folding has largely been elucidated in the case of thiolate coverage, the relationship between the atomic configuration and the most sensitive electronic structure deserves further inquiry. At the same time, the library of available well-characterized ligands should be expanded for CdTe NPLs. Most existing studies are devoted either to the synthesis and thermodynamics of their growth or to the study of the macroscopic optical properties of the films formed after the exchange [2,11,16,20].

In the work of Sun and Buhro, reversible ligand exchange from Z-type to L-type and back was realized for zinc-blended CdSe nanoplatelets, where $CdCl_2$ acts as a model halide Z-ligand, allowing to obtain well-defined compositions of the type $(CdSe)_3[CdCl_2]$ and fine-tune the lattice stress and the energy of edge transitions [21].

In this paper, we systematically investigate the impact of various ligand exchange strategies on the optical and structural properties of CdTe nanoplatelets. The primary objective of our study is to experimentally analyze the stability of colloidal CdTe nanoplatelets to postsynthetic ligand exchange under mild organic conditions. We explore the feasibility of adapting halide and sulfur-containing ligand exchange protocols, originally developed for CdSe nanoplatelets, to CdTe nanoplatelets and analyze the resulting optical and morphological changes. Particular attention is paid to the regimes in which exchange is ineffective or leads to morphological deterioration, as these conditions determine the applicability limits of these procedures for CdTe-based films.

Here we describe the comparison of three standard strategies borrowed from protocols for CdSe nanoplatelets, namely, replacement of the carboxylate shell with cadmium halide ($CdCl_2$), the use of zinc diethyldithiocarbamate ($Zn(DDTC)_2$), and a thiol ligand (hexadecanethiol). In our analysis, we determine the conditions under which no exchange occurs, particle degradation is observed, while regions of the 2D structure is maintained.

2. Material and methods

2.1. Chemicals

1-octadecene (ODE) (Sigma-Aldrich, 90%), propionic acid (Sigma-Aldrich, 99%), oleic acid (OA) (Sigma-Aldrich, 90%), cadmium acetate dihydrate ($Cd(OAc)_2 \cdot 2H_2O$) (> 98%), tellurium powder (Te) (98%), hexadecanethiol (Aldrich, > 95%), oleylamine (Aldrich, 70%), trioctylphosphine (Aldrich, 95%), hexane (> 99%), ethanol (95%), acetone (> 99%) dichloromethane (CH_2Cl_2) (> 99%), cadmium chloride ($CdCl_2$), methanol (CH_3OH).

2.2. Precursor preparation

Tellurium precursor TOP-Te

To prepare the tellurium precursor, 1 ml of trioctylphosphine (TOP) was added to 1 mmol (0.1276 g) of tellurium and dispersed using an ultrasonic bath until the tellurium powder is completely dissolved, resulting in a bright green solution.

Cadmium propionate $Cd(prop)_2$

To synthesize cadmium propionate, 8.07 mmol (2.15 g) of cadmium acetate $Cd(OAc)_2$ $2H_2O$ and 10 ml of propionic acid were placed in a 50 ml three-necked flask, the mixture was stirred at 90°C, and degassed for 1 hour under argon. After 1 hour, the mixture was removed from the heat, cooled, and then quenched with acetone at 50–60°C until it turned cloudy. A few minutes after adding acetone, a powder formed at the bottom, which was then filtered and dried. The result was a white powder of cadmium propionate.

2.3. Synthesis of CdTe NPLs with different concentrations

Synthesis of CdTe nanoplatelets with ± 50% variation of the cadmium precursor concentration: In a three-neck round-bottom flask, 0.195 g of cadmium propionate was loaded with 80 µL of oleic acid (OA) and 10 mL of 1-octadecene (ODE). The mixture was heated to 110°C under argon and kept at this temperature for 30 min under vigorous stirring to ensure degassing. The temperature was then raised to 170°C, and at this point 100 µl of a pre-prepared tellurium precursor solution diluted in 500 µl of octadecene was swiftly injected, resulting in an immediate color change of the reaction mixture to dark brown. After 20 min the heating mantle was removed, and at 150°C 1 mL of oleic acid was added to quench the growth of the CdTe nanoplatelets. The reaction mixture was subsequently cooled to room temperature and purified by precipitation with acetone (1:1 acetone to crude solution) followed by redispersion in a nonpolar solvent. For Cd-rich and Cd-poor conditions, the concentration of the cadmium precursor was varied by ± 50% relative to this standard procedure.

2.4. Ligand exchange from carboxylate to hexadecanethiol

A 2 mL aliquot of the as-prepared CdTe NPL dispersion (containing 4.2 µmol of Cd) was combined with 8 mL of hexane and 800 µL of hexadecanethiol, then stirred under an argon atmosphere for 30 min to remove dissolved gases. The mixture was subsequently heated to 65°C, after which 150 µL of oleylamine was injected and the reaction was maintained under stirring for 1 h. After cooling to room

temperature, the dispersion initially remained yellow; however, effective ligand exchange is typically accompanied by a red to dark-red color change. Therefore, the solution was kept for an additional 2 days to allow completion of the exchange, leading to a change in color from yellow to dark orange. The nanoplatelets were precipitated by adding acetone in a 1:1 ratio relative to the reaction mixture, collected by centrifugation at 18,000 rpm for 2 min, and finally redispersed in hexane.

2.5. Synthesis of CdTe NPLs by diethyldithiocarbamate ligand replacement

250 µl of the CdTe sample was taken, filled it with hexane to 1 ml (750 µl), and added 1 ml of a pre-prepared $Zn(DDTC)_2$ solution in toluene.

Preparation of $Zn(DDTC)_2$ in toluene: 0.09 g of the powder was dissolved in 10 ml of toluene (heated at low temperature with constant stirring).

There was no shift in the absorption peaks, indicating the absence of the diethyldithiocarbamate ligand. However, additional bands at 200–300 nm appeared, pertinent to the absorption of the ligand. These bands were not observed upon NPL purification. The sample was precipitated, redispersed in toluene, precipitated again, and dispersed in hexane, but no changes were observed.

2.6. Replacement of ligands with $CdCl_2$ for CdTe NPLs.

Ligand exchange with cadmium chloride ($CdCl_2$)

for the $CdCl_2$ ligand-exchange experiment, 500 µL (1 µmol Cd) of the CdTe nanoplatelet dispersion in hexane were first precipitated and the precipitate was redispersed in 1.5 mL of toluene. Then, 100 µL of oleylamine was added, followed by 200 µL of a $CdCl_2$ solution in methanol (prepared by dissolving 0.09 g of $CdCl_2$ in 10 mL of methanol, corresponding to 10 µmol of $CdCl_2$ in 200 µL). The resulting biphasic toluene/methanol mixture was left to stand for 10 min at room temperature to allow the two-phase ligand-exchange process to occur.

For ligand exchange in dichloromethane, 500 µL of the NPL sample was precipitated in 3 mL of a 1:2 solution of CH_2Cl_2 and methanol. After centrifugation, the process was repeated twice, and the precipitate was dispersed in 2 mL of dichloromethane. A solution of cadmium chloride in methanol was also added. The color changed from yellow to orange. Next, 1 mL of DMF was added and the mixture was centrifuged. After removing the thin film, the precipitate was dissolved in a solution of dichloromethane and ethanol and reprecipitated. Finally, the precipitate was redispersed in 2 mL of CH_2Cl_2.

2.7. Material characterization

The UV-Vis absorption spectra of the NPLs was recorded using a Jasco V-770 spectrophotometer in the range of 200–800 nm, while FTIR spectra were collected using a JASCO FT/IR-4700 spectrometer at

room temperature. Photoluminescence (PL) was measured using a Solar CM 2203 and Edinburgh FLS1000 spectrofluorimeter (PL and PLQY) in quartz cuvettes. Chemical analysis were carried out and the elemental composition of CdTe NPL was studied using the TXRF method on the S2 Picofox device (Bruker), excitation by Mo Kα radiation, voltage 50 kV. The NPL dispersions were dried on sapphire substrates. As a result of the analysis, the absolute masses of the elements in the sample were determined, and the concentrations of cadmium and tellurium in the used sols were refined. After synthesis, all nanoplatelet samples were purified twice by precipitation and redispersion, and then stored as purified dispersions in hexane. Before the TXRF analysis, we first evaluated whether additional purification cycles could affect the measured Cd/Te ratio, the data are shown in the Supporting Information (Table S2). The results showed that two further purification cycles did not lead to any significant change in the TXRF-derived Cd/Te values. Therefore, for the final measurements, the twice-purified nanoplatelet dispersions were subjected to one additional purification step immediately before deposition onto sapphire substrates.

Electron microscopy and electron diffraction studies were conducted using a JEM-2100 (JEOL) TEM, equipped with a LaB6 gun and an 11-megapixel Quemesa CCD camera (Olympus). The accelerating voltage was set to 200 kV. Hexane sols containing NPLs were deposited onto carbon-coated copper grids and dried. The grids were then etched in argon plasma to remove organic material before examination. The sizes of the NPLs were manually measured from micrographs using Image-Pro Plus 6.0 software.

3. Results and discussion

To study the effect of precursor concentration on the growth and optical properties of NPLs, CdTe nanoplatelets were synthesized using different precursor concentrations. The concentrations of cadmium and tellurium precursors were increased or decreased by 50% relative to our previously reported synthesis protocol (Table S1) [11]. Absorption and luminescence spectra were measured to study the changes in the exciton peaks of CdTe NPLs, which should correspond to peaks at 450 nm and 500 nm, indicating a thickness of 3ML. The obtained spectra are shown in Fig. 1.

Figure 1 (a, b, c, d) shows a series of absorption spectra of CdTe samples synthesized at 170°C with + 50%, -50% excess and deficiency of cadmium and tellurium, and a comparison of the curves corresponding to different aliquot sampling times (10 s, 30 s, 1 min, 5 min, 10 min), showing the evolution of the spectra over time. At short times (10–30 s), the absorption is weakly expressed, the peaks are smoothed, indicating the initial stage of nanoparticle formation. As the synthesis time increases (1–10 min), the peak intensity increases, and the lines become more pronounced, which is associated with the growth and ordering of nanoplatelets.

Our study showed that CdTe nanoplatelets exhibit a narrow Cd/Te stoichiometry variation when the reaction mixture is relatively Cd-deficient (-50%Cd), where the system immediately enters a supersaturation state – the nucleation of the target 3 ML NPLs occurs within ~ 10 seconds after

injection, without noticeable intermediate stages. With an excess of precursors (+ 50%), growth slows for 3–10 minutes, accompanied by the formation of intermediate phase states. The literature emphasizes that the growth processes and thickness control of CdTe nanoplatelets remain much less well-studied than similar phenomena in CdSe-based systems, despite individual publications devoted to the synthesis and improvement of their properties [3,4]. Furthermore, it has been established that the rate of precursor conversion and the availability of monomers play a decisive role in the formation and development of colloidal nanocrystals. However, precisely establishing the optimal time range for the direct formation of nanoplatelets of a precisely specified thickness remains an unresolved problem [22].

The precursor-composition dependence in Fig. 1 shows relative to the starting synthesis protocol used in this work. The labels Cd + 50% and Cd − 50% denote changes relative to this starting protocol. Therefore, the faster appearance of the characteristic CdTe NPL absorption features in the Cd − 50% sample does not imply that Cd deficiency generally accelerates nucleation. Rather, it suggests that the starting protocol may contain an excess of Cd-containing species, and that reducing the Cd precursor amount shifts the reaction mixture closer to a more favorable Cd/Te balance for the formation of 3 ML CdTe NPLs.

Thus, the observed trend is considered a comparative result within the studied precursor-composition series. The data show that, depending on the precursor ratio, the characteristic optical features of 3 ML CdTe NPLs can appear within the first seconds of synthesis at 170°C. In addition, the relative Cd/Te balance affects the rate at which the characteristic absorption peaks of the 3 ML NPL population emerge.

The most pronounced spectral characteristics, are observed for the samples synthesized within 10 minutes, indicating a fully completed crystallization process and the achieved stable morphology of the CdTe nanostructures. Therefore, the obtained spectra demonstrate the influence of reaction time on the optical properties of CdTe NPLs and confirm the importance of the growth dynamics and stabilizing the colloidal system. The absorption (black) and photoluminescence (red) spectra of the CdTe nanoplatelets are shown in Fig. 2.

Figure 2 shows the optical absorption (black curves) and photoluminescence (red curves) spectra of CdTe nanoplatelets synthesized at 170°C with different precursor stoichiometries: (a) + 50% excess cadmium, (b) − 50% deficiency of cadmium, (c) + 50% excess tellurium, (d) − 50% deficiency of tellurium. The graph shows that in all cases, the absorption spectra have pronounced peaks corresponding to exciton transitions at 450 nm electron-light hole and at 500 nm electron-heavy hole in CdTe nanoplatelets, which proves the growth of the NPL. The most intense absorption maximum is recorded in the range of ~ 500 nm. The luminescence spectra excited at 450 nm, clearly show an intense narrow peak at 501 nm, with a Stokes shift of 1 nm for all samples (Fig. 2a, b, c, d). With a cadmium deficiency (–50% Cd, Fig. 2b), the position of the main PL maximum remains in the same spectral region, but a noticeable enhancement of the long-wavelength part of the spectrum is observed.

Figure 2b shows the luminescence spectra of a sample containing – 50% cadmium, measured on different spectrofluorimeters. The blue curve corresponds to a spectrum obtained one year ago on a Solar CM2203. The red and purple curves represent newly repeated measurements of a previously synthesized sample stored for approximately one year, recorded using the CM2203 and Edinburgh FLS1000 spectrofluorometers, respectively. The only difference was in the position of the luminescence maximum: on the older CM2203 spectrofluorimeter, it was recorded at around 506 nm, whereas on the newer FLS1000, the maximum was observed at 501 nm. Apart from this minor difference in the peak position and instrumental artefact observed near 525 nm, the spectra were essentially identical, indicating that the measurements performed one year earlier were reliable and reproducible. It is also clear that the sample has undergone degradation over the course of one year. The long-wavelength emission, which was less pronounced in the freshly prepared sample, became more evident after one year, forming a broad emission band in the 520–650 nm range.

The evolution of PL spectra after 12 months suggests that the sample 2 showing the fastest formation of the target CdTe NPL population is less optically stable during storage. In this sample, the emission feature around 553 nm becomes more pronounced, together with an additional band near 585 nm and a broad red-emission tail. According to the literature [23], CdTe NPLs can form discrete thickness populations with excitonic transitions around 428, 500, and 556 nm, and the 553 nm band corresponds to a thicker NPL population. Therefore, the increased emission around 553 nm may indicate the emergence or enhanced contribution of thicker NPLs. At the same time, the broad low-energy emission may be associated with surface- or deep-trap-related states.

In contrast, samples 1, 3, and 4 show more stable photoluminescence, with only a minor contribution from the thicker NPL population. This suggests that the initial precursor concentration does not only control the apparent rate of NPL maturation, but also affects the long-term optical stability of the resulting NPL ensemble.

In the present case, Cd-deficient conditions appear to create a narrow kinetic window for rapid formation of the target 3 ML CdTe NPL population. However, after prolonged storage, the PL spectrum changes, indicating reduced optical stability. One possible explanation is that rapid growth under Cd-deficient conditions leads to less robust surface passivation and a higher probability of surface-related emissive states. In contrast, Cd-rich or moderately Cd-rich conditions may slow down the maturation process but provide a more favorable environment for stable NPL growth and surface stabilization.

Based on this interpretation, a two- or three-step precursor-addition strategy may be considered. An initial Cd-deficient stage could promote rapid formation of the target NPL population, followed by controlled Cd addition to improve surface passivation and suppress the formation of defect-related emission during storage.

For these samples, it was interesting to study the stoichiometry and cadmium-to-tellurium ratio using XRF. For this purpose, 500 µL of sample were precipitated and dissolved in 100 µL of hexane, dispersed in an ultrasonic bath, and then 3 µL of each sample were dropped onto a sapphire substrate. The

elemental composition of the purified CdTe nanoplatelets was analyzed using XRF and is shown in Table 1.

Table 1
Elemental composition of purified CdTe nanoplatelets

Sample	Mass (Cd), ng	Mass (Te), ng	Ratio of elements
CdTe-Cd + 50%	1423	1199	1.19
CdTe-Cd-50%	1850	1799	1.03
CdTe-Te + 50%	1544	1444	1.07
CdTe-Te-50%	1322	1236	1.07

Table 1 lists the mass amounts of Cd and Te for samples synthesized at 170°C with varying initial stoichiometry of the precursors (Cd ± 50%, Te ± 50%). In all cases, the Cd/Te ratio slightly exceeds unity.

Using a 50% excess of cadmium (Cd/Te ≈ 1.19) indicates a significant enrichment of the nanoplatelets with cadmium. When the cadmium content was reduced to -50% their ratio approached unity (≈ 1.03), indicating a more complete incorporation of available cadmium into the material and increased efficiency of precursor use in a first second of the growth.

In the sample with excess tellurium (+ 50%) Cd/Te ratio is ≈ 1.07. Despite the increased concentration of Te, the final material shows moderate cadmium enrichment, confirming the role of cadmium-containing complexes in stabilizing growing nanoplatelets. In the case of tellurium deficiency (-50%), the ratio of Cd/Te ≈ 1.07 remains unchanged comparing with the excess of tellurium.

The nearly unchanged Cd/Te ratio after TXRF analysis may indicate that the purification procedure efficiently removes unreacted or weakly bound precursor species. Therefore, the measured composition reflects the purified CdTe NPL fraction rather than the initial precursor stoichiometry. At the same time, the optical differences between the samples suggest that precursor concentration still influences the growth pathway and defect/surface-state formation.

The FTIR spectra of CdTe nanoplatelets before and after post-synthetic ligand exchange: the initial sample with a carboxylate shell (CdTe), samples after treatment with hexadecanethiol (CdTe + HDT), $CdCl_2$ (CdTe+$CdCl_2$) and zinc diethyldithiocarbamate (CdTe + $Zn(DDTC)_2$) are shown in Fig. 3.

In all cases, a set of bands characteristic of alkyl carboxylate ligands is present: C–H stretching vibrations in the range of 2800–3000 cm^{-1} and deformation bands at 1460 and 1520 cm^{-1}, with significant changes in the spectrum observed only for the CdTe + HDT sample. IR spectroscopy data further confirm the different efficiencies of the ligand exchange methods used (Fig. 3). The spectrum of the original CdTe nanoplatelets clearly displays bands corresponding to the stretching vibrations of methylene groups in the region of 2800–3000 cm^{-1}, as well as a complex set of bands in the range of 1400–1600 cm^{-1}, responsible for the asymmetric and symmetric vibrations of the carboxylate group.

After treatment with thiol, the vas(CH3) vibration is enhanced, indicating surface coverage with thiol. The vas(COO-) and vs(COO-) vibrations, which are responsible for the carboxylate ligands, are clearly visible in the original CdTe sample and in samples with cadmium chloride and zinc diethyldithiocarbamate. After replacement with thiol, the vs(COO-) vibrations disappear in the spectrum, while the vas(COO-) vibrations become less noticeable, confirming a successful replacement from carboxylate to thiolate. After treatment with $CdCl_2$ and $Zn(DDTC)_2$ solutions, the shape and relative intensity of the bands remain virtually unchanged, with only the appearance of weak additional features characteristic of the reagents themselves. These data are consistent with the optical results and indicate that, under the conditions used, cadmium chloride and zinc diethyldithiocarbamate do not significantly displace the original carboxylate shell on the surface of the CdTe nanoplatelets. The infrared spectrum of the CdTe + HDT sample differs significantly from the original: enhanced alkyl chain stretching bands, a change in the structure of the "carboxylate" range of 1400–1600 cm^{-1}, and the emergence of new features in the low-frequency region indicate changes in the composition of the organic coating after the addition of hexadecanethiol. Together with the observed shifts of exciton transitions, photoluminescence decay and broadening, and the observed folding of nanoplatelets into scrolls in TEM images, the FT-IR spectroscopy data confirm that the thiol group actually interacts with the surface of CdTe nanoplatelets, whereas exchange reactions involving $CdCl_2$ and $Zn(DDTC)_2$ practically do not occur under mild organic conditions.

To study the influence of different ligand exchange conditions on the properties of colloidal semiconductor CdTe nanoplatelets, another series of ligand exchange experiments was conducted. First, a postsynthetic ligand exchange was performed from carboxylate to halide $CdCl_2$. The absorption spectrum of CdTe nanoplatelets after postsynthetic treatment with a $CdCl_2$ solution in a toluene/dichloromethane system in the presence of oleylamine is shown in Fig. 4.

Figure 4 shows the optical absorption spectra of CdTe nanoplatelets after attempted ligand exchange from the carboxylate shell to cadmium halide dispersed in toluene and dichloromethane. The heavy- and light-hole excitonic peaks at ~ 450 and ~ 500 nm correspond to the peak positions of standard CdTe nanoplatelets and retain their relative intensity and linewidth, indicating the absence of a halide shell on the nanoplatelets and an unsuccessful ligand exchange. It was impossible to record optical photoluminescence spectra for these CdTe nanoplatelets with the ligand changed to $CdCl_2$, since the nanoplatelets degraded and precipitated in a two-phase solution a few hours after postsynthetic ligand exchange, turning black. The difference in polarity between methanol and toluene leads to the formation of a two-phase system in which the ligand exchange of carboxylates for chloride anions is accompanied by a change in the polarity of the nanoplatelet surface and their redistribution between the phases. Partial precipitation is associated with a temporary loss of colloidal stability during the transition between polar and non-polar environments. Dufour et al. showed that successful carboxylate → halide exchange on CdSe NPLs requires not only an excess of halide ions but also costabilization of the surface with primary amines, which relieves elastic stresses in the crystal lattice and leads to a noticeable red shift and an increase in emission brightness [24]. Halide ligand exchange methods are

widely used for CdSe nanoplatelets, but they remain poorly studied for CdTe NPLs. This is due to differences in surface chemistry and the higher susceptibility of CdTe to destabilization in polar environments, which limits the formation of a uniform and stable halide shell. The results demonstrate the high stability of the carboxylate shell of CdTe NPLs to substitution with cadmium chloride, while the applied conditions ensure only partial desorption of organic ligands without the formation of stable halide passivation. As can be seen in the Fig. 4, a clear peak at 514 nm appears when toluene is used as the solvent. No additional peaks are observed during ligand exchange when CdTe nanoplatelets are dispersed in dichloromethane. Differences in solvent polarity can affect the spectral characteristics of CdTe-NPLs, leading to the appearance of additional features in the optical spectra in some environments and their smoothing in others; this behavior was studied in [24]. For CdTe nanoplatelets, the wurtzite and zinc blend modifications exhibit significantly different reactivity in ligand exchange reactions, which the authors attribute to differences in the set and polarity of active facets; this emphasizes that the efficiency of carboxylate → halide exchange in CdTe-NPL systems is sensitive to the crystal structure of the core [13].

Against this background, the absence of a noticeable shift of the exciton peaks and a change in the shape of the spectrum in CdTe NPLs samples after treatment with a $CdCl_2$ solution (Fig. 4) indicates that under our conditions either no significant exchange of carboxylate ligands for cadmium chloride occurs, or it is limited to a small number of defect centers and does not lead to the formation of a continuous halide shell.

The next ligand exchange on CdTe nanoplatelets was performed from carboxylate to thiolate using hexadecanethiol. A study of the effect of thiol groups on the optical properties of the nanoplatelets revealed a noticeable shift of the exciton peaks toward longer wavelengths, from 450 nm to 476 nm for electron-light holes and from 500 nm to 530 nm for electron-heavy holes, by 26 and 30 nm, respectively. A broadening of the absorption bands and a decrease in the intensity of the exciton peaks are also noted. The absorption and photoluminescence spectra of CdTe nanoplatelets after postsynthetic exchange of carboxylate ligands with hexadecanethiol are shown in Fig. 5.

The presence of two excitonic features indicates quantum size effects and the polydispersity of the particles in the system. Thus, the spectrum confirms the formation of colloidal CdTe nanoplatelets with a size distribution and a characteristic quantum size shift in the visible range.

The Fig. 5 (blue curve) shows the photoluminescence spectrum of sample, measured in the 500–600 nm range. The blue spectrum indicates luminescence after using hexadecanethiol for ligand replacement. After treatment with hexadecanethiol, the PL maximum shifts to 527 nm. This peak shift indicates successful replacement, while maintaining the luminescent properties. Furthermore, as can be seen from the absorption spectrum for the same sample (Fig. 5, red curve), exciton features in the 476 and 530 nm range are preserved, consistent with the preservation of the two-dimensional structure of the nanoplatelets. Thus, thiol treatment leaves the quantum-size parameters of CdTe NPLs virtually unchanged, but leads to a noticeable change in the energy and emission efficiency.

Replacing the carboxylate shell with hexadecanethiol results in a significant weakening of photoluminescence, an increase in the spectral line width and its asymmetry (Fig. 5). This effect is consistent with data obtained previously for CdSe nanoplatelets and nanocrystals with a thiol shell [25,26], where a decrease in intensity and a broadening of the band were explained by the formation of shallow surface traps and a change in the phase relaxation time (Fig. 5). Similarly, the observed changes in the photoluminescence parameters of CdTe NPLs after treatment with hexadecanethiol indicate an increase in the structural and energetic inhomogeneity of the surface compared to the initial carboxylate coating.

The PLQY values were measured after approximately one year of storage: therefore, they should not be interpreted as the initial quantum yields of the freshly synthesized samples. The pristine CdTe NPLs showed a PLQY of 3.86%, whereas the HDT-treated sample exhibited a lower value of 1.78%. Although the absence of PLQY measurements immediately after synthesis does not allow us to quantify the extent of aging-induced degradation, the retained measurable PLQY suggests that the samples preserved detectable photoluminescent activity after long-term storage.

Replacing the ligands in CdTe NPLs with thiols causes controlled folding and formation of the CdS layer, enabling the control of the shape of two-dimensional structures and the production of folded heterostructures with tuned optical properties. TEM images of the initial NPLs and those after ligand exchange with a thiolate are shown in Fig. 5b,c.

Figure 5b shows distinct rectangular nanoplatelets with sharp edges, maintaining their two-dimensional shape with minimal edge degradation. Figure 5c shows numerous curved and scrolled nanoplatelets. It is evident from the figure that a significant portion of the NPL has lost its original rectangular shape and has undergone mechanical deformation and scrolling. Many platelets bend along their length, forming tubular or arcuate fragments. This scrolling indicates that thiol treatment affects not only the composition of the surface shell but also the mechanical state of the nanoplatelets, leading to a significant restructuring of their shape.

Conclusion

In this study, we conducted a comprehensive analysis of the optical and structural characteristics of colloidal cadmium telluride nanoplatelets, as well as their stability to ligand exchange after synthesis under mild organic conditions. It was found that at a temperature of 170°C, with variations in cadmium and tellurium concentrations within ± 50%, nanoplatelets with a thickness of approximately 3 monolayers were always formed, with a pronounced pair of exciton transitions at wavelengths of 450 and 500 nm, as well as a narrow photoluminescence band at 501 nm. Post-synthetic ligand exchange using $CdCl_2$ and $Zn(DDTC)_2$ has virtually no effect on exciton transitions in CdTe nanoplatelets: treatment with $CdCl_2$ solution leaves the spectral positions of the maxima unchanged, but causes a loss of dispersion stability and particle precipitation, while the addition of $Zn(DDTC)_2$ does not produce intrinsic complex bands in the UV region with an unchanged exciton part of the spectrum and FTIR spectroscopy of the carboxylate shell, which indicates the absence of effective exchange between carboxylate and

diethyldithiocarbamate ligands under these conditions. Analysis of the results of all three types of ligand substitution allows us to construct a “stability map” of CdTe NPLs in the coordinates “ligand type – observed effect.”

At the same time, hexadecanethiol can significantly alter the optical properties and exhibit strong interactions with the surface, but is accompanied by twisting and aggregation of the nanoplatelets. Consequently, the feasible surface modification space for CdTe nanoplatelets without loss of their two-dimensional structure is significantly narrower than expected based on experiments with CdSe nanoplatelets. These data demonstrate the importance of developing specialized, gentle ligand exchange techniques adapted specifically for CdTe-based materials and can serve as a guide when selecting processing parameters for film structures based on them for use in optoelectronic devices.

In addition, we identified a stoichiometric supersaturation window in which CdTe nanoplatelets with the target ~ 3 ML thickness were formed already within the first seconds of growth, as evidenced by the rapid appearance of the characteristic excitonic absorption features near 450 and 500 nm. This provides a practical basis for controlling CdTe NPL thickness at the early stage of synthesis. PLQY measurements further confirmed that the optical quality of the nanoplatelets is strongly dependent on post-synthetic surface treatment, highlighting the need for carefully controlled ligand-exchange conditions to preserve excitonic emission.

Declarations

Author Contributions

Conceptualization, D.D., S.B., and R.D.; Funding acquisition, D.D.; Investigation, S.B., A.O., S.D., and E.K.; Methodology, S.D. and A.O.; Project administration, D.D.; Resources, D.D. and S.D.; Supervision, D.D., S.B., and R.D.; Validation, R.D., M.S.K., and A.A.; Visualization, M.S.K. and A.O.; Writing – original draft preparation, A.O., D.D., and S.B.; Writing – review and editing, A.V., A.K., D.D., and S.B. All authors have read and agreed to the published version of the manuscript.

Funding

The part of this research performed by the group from ENU (material and nanoplatelets synthesis, optical measurements) was funded by the Science Committee of the Ministry of Science and Higher Education of the Republic of Kazakhstan (Grant No. AP23490788). The work of the group from MSU (XRF and IR spectroscopy) was supported through the Lomonosov Moscow State University Program of the Development within state contract AAAA-A21-121011590082-2.

Data Availability Statement

The original contributions presented in the study are included in the article; further inquiries can be directed to the corresponding authors.

Acknowledgments

The authors acknowledge support from M. V. Lomonosov Moscow State University Program of Development in the form of access to a Frontier FTIR spectrometer and an S2 Picofox TXRF spectrometer.

Conflicts of Interest

The authors declare no conflicts of interest.

References

1. Singh, S. et al. Colloidal CdSe Nanoplatelets, A Model for Surface Chemistry/Optoelectronic Property Relations in Semiconductor Nanocrystals. *J. Am. Chem. Soc.* **140**, 13292–13300 (2018).
2. Hu, A. et al. Colloidal II–VI nanoplatelets for optoelectronic devices: Progress and perspectives. *Nano Res.* **17**, 10412–10425 (2024).
3. Ithurria, S. et al. Colloidal nanoplatelets with two-dimensional electronic structure. *Nat. Mater.* **10**, 936–941 (2011).
4. Diroll, B. T. et al. 2D II–VI Semiconductor Nanoplatelets: From Material Synthesis to Optoelectronic Integration. *Chem. Rev.* **123**, 3543–3624 (2023).
5. Fang, W. et al. Emergence of colloidal quantum well-based optoelectronics. *Cell. Rep. Phys. Sci.* **5**, 101936 (2024).
6. Kainarbay, A. et al. Synthesis and Luminescence Dynamics of CdSe and CdSe/CdS Quantum Dots. *Eurasian J. Phys. Funct. Mater.* **9**, 1–1 (2025).
7. Daouda, T., Nya, F., Dzifack Kenfack, G. M., Laref, A. & Mohamadou, A. Multilayers strategy with a mixed CdTe/ZnTe absorber layer for optical trapping and efficiency improvement in CdTe-based solar – SCAPS modelling. *Phys. Scr.* **99**, 055964 (2024).
8. Anand, A. et al. Optical and Scintillation Properties of Record-Efficiency CdTe Nanoplatelets toward Radiation Detection Applications. *Nano Lett.* **22**, 8900–8907 (2022).
9. Laboratory, A. P. Department of Physics, Savitribai Phule Pune University, Pune – 411007 et al. Cadmium Telluride/Cadmium Sulfide Thin Films Solar Cells: A Review. *ES Energy Environ.* (2020). https://doi.org/10.30919/esee8c706 doi:10.30919/esee8c706.
10. Akhmetova, A. et al. Effect of Nanoplatelets Thickness on Photoluminescent, Optical, and Electronic Properties of Synthesized CdTe Semiconductor Nanoplatelets. *Crystals* **13**, 1450 (2023).
11. Ospanova, A. et al. Investigation of the Influence of Structure, Stoichiometry, and Synthesis Temperature on the Optical Properties of CdTe Nanoplatelets. *Nanomaterials* **14**, 1814 (2024).
12. Koshkinbayev, Y. et al. The Influence of Temperature and Stoichiometry on the Optical Properties of CdSe Nanoplatelets. *Nanomaterials* **14**, 1794 (2024).

13. Sun, H. & Buhro, W. E. Contrasting Ligand-Exchange Behavior of Wurtzite and Zinc-Blende Cadmium Telluride Nanoplatelets. *Chem. Mater.* **33**, 1683–1697 (2021).
14. Jin, X., Parisi, J. & Kolny-Olesiak, J. Shape Control of CdTe Nanocrystals: Influence of the Solvent Composition and Ligand Effects. *J. Nanopart.* **2013**, 1–7 (2013).
15. Silva, F. O. et al. Effect of surface ligands on the optical properties of aqueous soluble CdTe quantum dots. *Nanoscale Res. Lett.* **7**, 536 (2012).
16. Vasiliev, R. B. et al. Spontaneous Folding of CdTe Nanosheets Induced by Ligand Exchange. *Chem. Mater.* **30**, 1710–1717 (2018).
17. Swift, M. W., Efros, A. L. & Erwin, S. C. Controlling light emission from semiconductor nanoplatelets using surface chemistry. *Nat. Commun.* **15**, 7737 (2024).
18. Martinet, Q. et al. Ligand-dependent nano-mechanical properties of CdSe nanoplatelets: calibrating nanobalances for ligand affinity monitoring. *Nanoscale* **13**, 8639–8647 (2021).
19. Elimelech, O. et al. Entropy of Branching Out: Linear versus Branched Alkylthiols Ligands on CdSe Nanocrystals. *ACS Nano*. **16**, 4308–4321 (2022).
20. Bubenov, S. et al. Observation of Direct and Indirect Effects of Surface Stabilizer on the Attenuation Coefficient of CdTe Nanoplatelet Films. *Nanomaterials* **15**, 1688 (2025).
21. Sun, H. & Buhro, W. E. Reversible Z-Type to L-Type Ligand Exchange on Zinc-Blende Cadmium Selenide Nanoplatelets. *Chem. Mater.* **32**, 5814–5826 (2020).
22. Owen, J. S., Chan, E. M., Liu, H. & Alivisatos, A. P. Precursor Conversion Kinetics and the Nucleation of Cadmium Selenide Nanocrystals. *J. Am. Chem. Soc.* **132**, 18206–18213 (2010).
23. Pedetti, S. et al. Optimized Synthesis of CdTe Nanoplatelets and Photoresponse of CdTe Nanoplatelets Films. *Chem. Mater.* **25**, 2455–2462 (2013).
24. Dufour, M. et al. Halide Ligands To Release Strain in Cadmium Chalcogenide Nanoplatelets and Achieve High Brightness. *ACS Nano*. **13**, 5326–5334 (2019).
25. Ahmed, T. et al. Hetero-confinement in single CdTe nanoplatelets. Preprint at (2024). https://doi.org/10.26434/chemrxiv-2024-85hg8
26. Antanovich, A. et al. A strain-induced exciton transition energy shift in CdSe nanoplatelets: the impact of an organic ligand shell. *Nanoscale* **9**, 18042–18053 (2017).

Figures

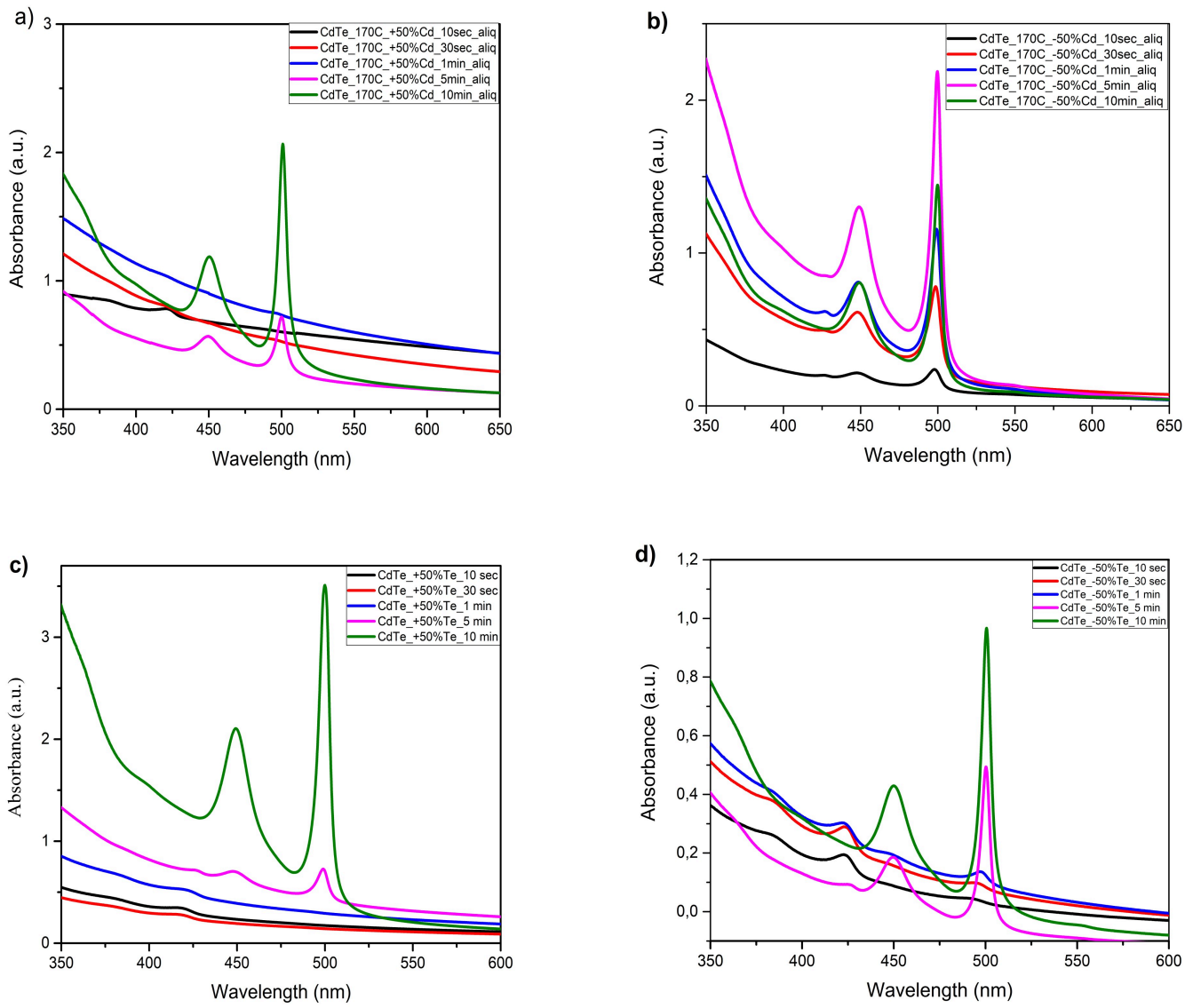


Figure 1

Absorption spectra of aliquots and initial CdTe NPLs with increased and decreased by 50% cadmium and tellurium precursors: a) for NPLs with an excess of cadmium +50%; b) with a deficiency of cadmium -50%; c) with an excess of tellurium +50%; d) with a deficiency of tellurium -50%.

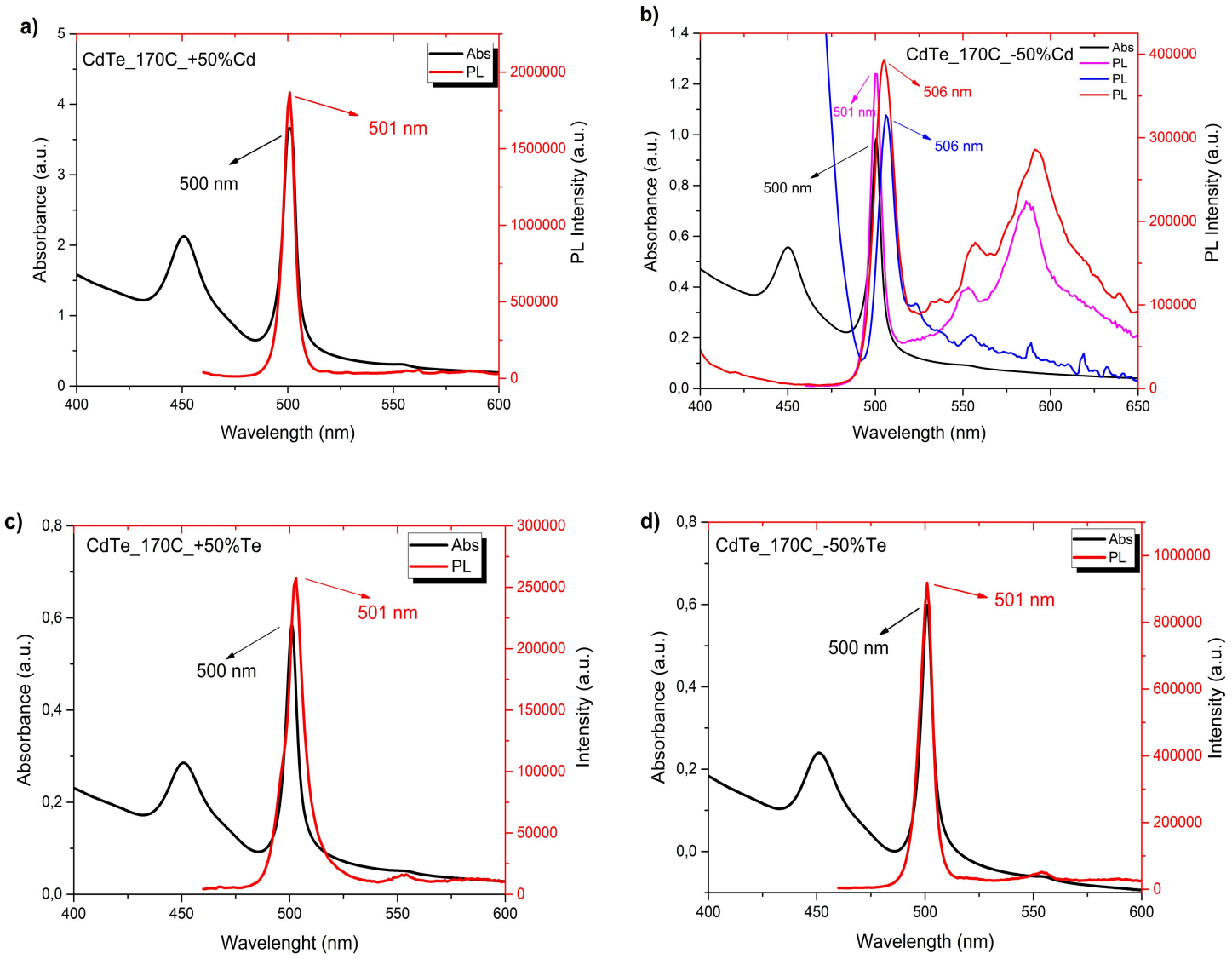


Figure 2

Absorption (black line) and luminescence (red line) spectra of cadmium telluride NPL

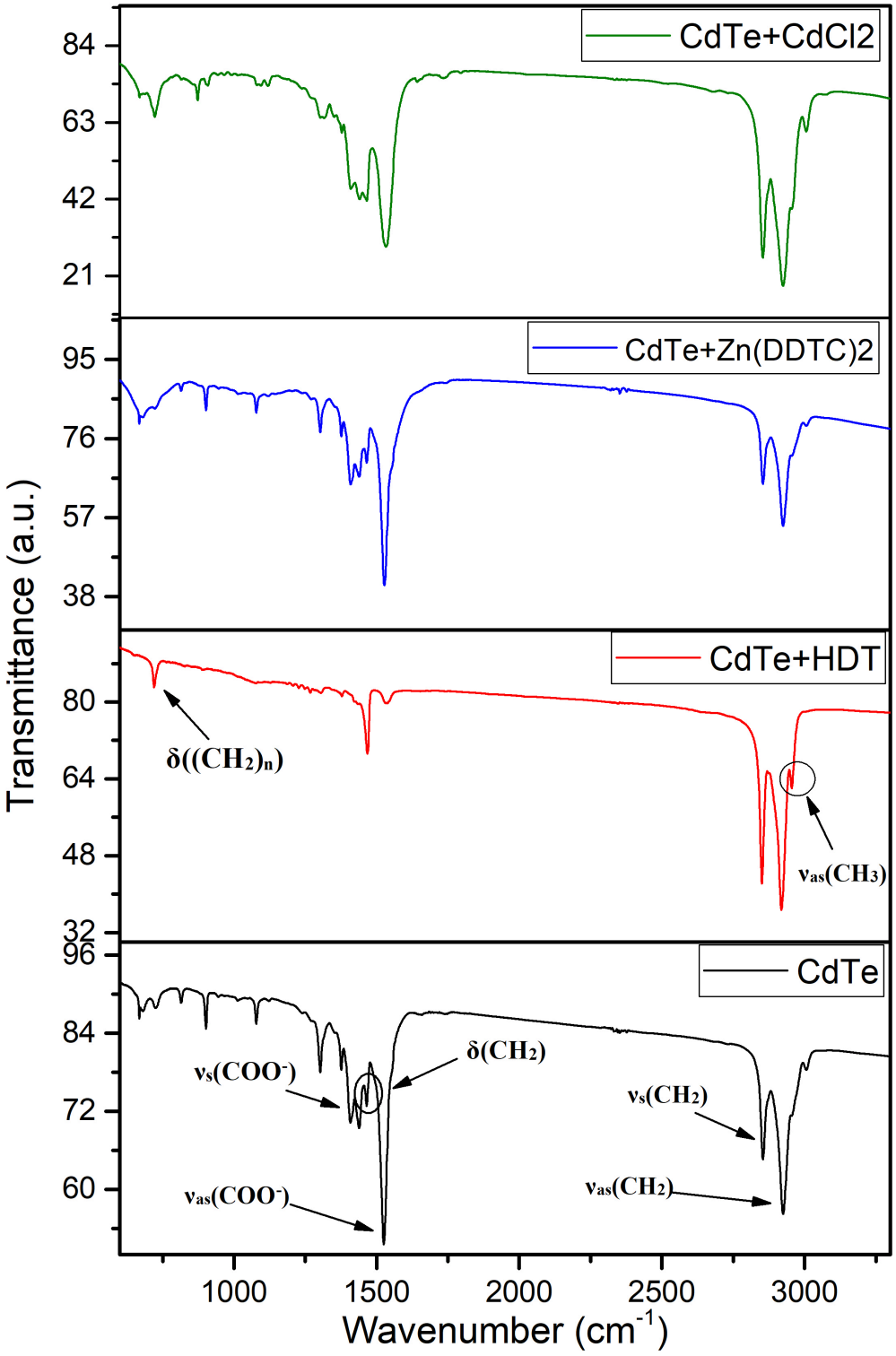


Figure 3

IR spectra for CdTe NPLs treated with different types of ligand: *black curve – initial NPL, red curve – with hexadecanethiol, blue curve – with zinc diethyldithiocarbamate, green curve – with cadmium chloride halide.*

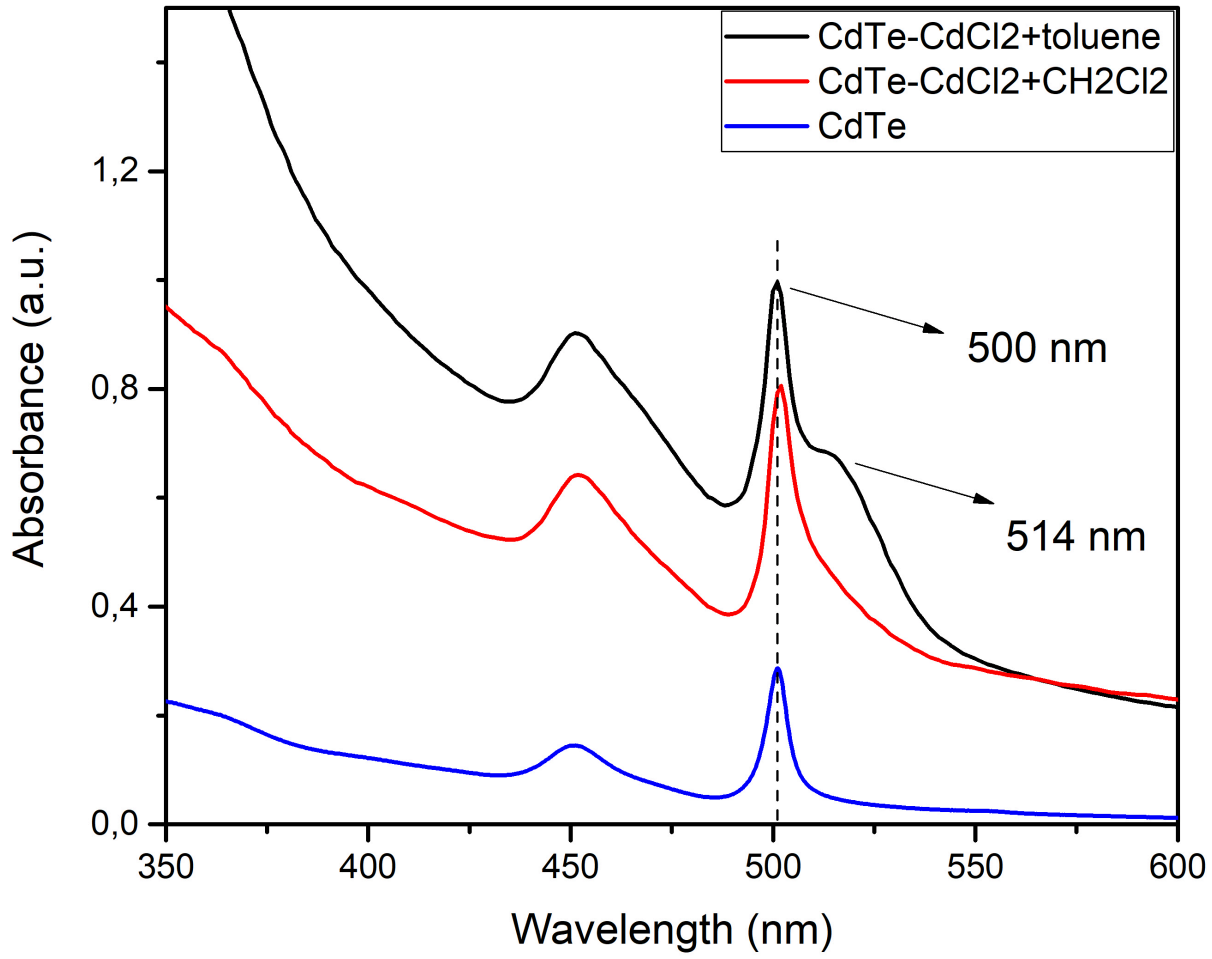


Figure 4

Absorption spectrum of CdTe nanoplatelets after postsynthetic ligand exchange from carboxylate to halide $CdCl_2$: a) in toluene; b) in dichloromethane.

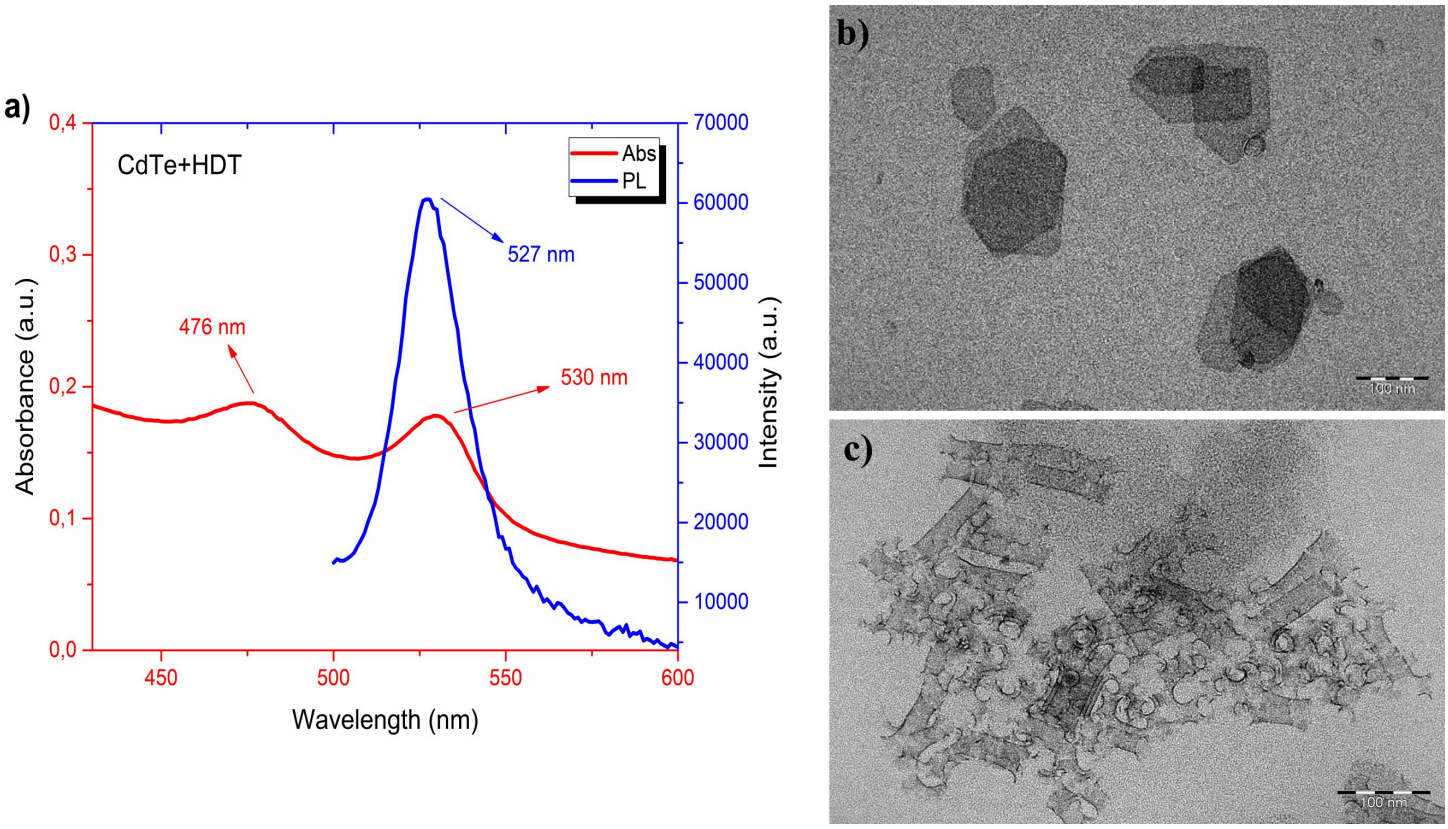


Figure 5

Optical and morphological characterization of CdTe NPLs replaced with a thiol ligand instead of a carboxylate: a) absorption and photoluminescence spectra of CdTe+HDT; b) TEM image of the as-prepared CdTe NPLs; c) TEM image of the CdTe NPLs after treatment with hexadecanethiol.

Supplementary Files

This is a list of supplementary files associated with this preprint. Click to download.

- Supportinginformation.pdf